CATALOGED BY DDC
AS AD No. 406879

406 879

ARPA ORDER NO. 189-61

MEMORANDUM
RM-3649-ARPA
MAY 1963

A SIMPLIFIED MODEL OF THE LAMINAR WAKE OF A HYPERSONIC BODY FOR STUDYING ELECTROMAGNETIC EFFECTS

R. D. Engel

PREPARED FOR:
ADVANCED RESEARCH PROJECTS AGENCY

The RAND Corporation
SANTA MONICA • CALIFORNIA

NO OTS

BEST
AVAILABLE COPY

PREFACE

The work described in this Memorandum was pursued in connection with a study of radar reflection and absorption characteristics of the wake of a re-entry vehicle. The study is one of a series related to the ICBM discrimination problem currently being pursued at RAND under the sponsorship of the Advanced Research Projects Agency.

SUMMARY

The problem of the absorption and reflection of electromagnetic energy from the wake of a body moving at hypersonic speed through the atmosphere has engaged the attention of a number of researchers in the defense community. In connection with that problem, this paper presents a simplified analytical model for investigating such wake characteristics as electron density, collision frequency, velocity, and temperature. Thus, the model furnishes the information which is necessary for studying the electromagnetic scattering properties of the wake.

The model is based on the work of Paul Lykoudis, and assumes inviscid laminar flow about a blunt body. A simplified expression for the enthalpy in the wake is derived from Lykoudis' universal solution. The enthalpy is then translated into the desired wake characteristics by using the equilibrium properties of air. For simplicity the air is assumed to be in local equilibrium. This represents an approximation since the air is strictly in local equilibrium only at lower altitudes where the wake is turbulent.

A particular set of re-entry conditions is considered as an example, and an analytical expression for the electron density is derived. This expression is compared with the electron density contours derived in previous studies elsewhere, and the differences are discussed. Finally the general structure of the wake is illustrated by plotting electron density contours.

ACKNOWLEDGMENTS

The author wishes to express his appreciation and thanks to Paul Lykoudis, consultant to The RAND Corporation, and to Mary Romig, Robert Kirkwood, and Patrick Benson of The RAND Corporation for many helpful comments and suggestions.

CONTENTS

PREFACE iii

SUMMARY v

ACKNOWLEDGMENTS vii

LIST OF FIGURES xi

LIST OF SYMBOLS xiii

Section

I. INTRODUCTION 1

II. GENERAL DISCUSSION OF THE WAKE 2

III. SIMPLIFIED MODEL OF THE CONDUCTION REGION OF THE WAKE 7

IV. DETERMINATION OF THE WAKE PROPERTIES FROM THE SIMPLIFIED MODEL 11

V. CONCLUSIONS 25

Appendix

A. ARDC MODEL ATMOSPHERE 26

B. PROPERTIES OF EQUILIBRIUM AIR 33

REFERENCES 42

LIST OF FIGURES

1. Structure of the hypersonic wake 3
2. Typical re-entry trajectories 12
3. Radial electron distribution 20
4. Axial electron distribution 21
5. Electron density profiles (Case 1) 23
6. Electron density profiles (Case 2) 24

(Appendix A--ARDC MODEL ATMOSPHERE)

7. Enthalpy 27
8. Density 28
9. Pressure 29
10. Log pressures 30
11. Speed of sound 31
12. Temperature 32

(Appendix B--PROPERTIES OF EQUILIBRIUM AIR)

13. Entropy 34
14. Density 35
15. Log density 36
16. Temperature 37
17. Compressibility factor 38

18a. Electron density 39

18b. Electron density 40

19. Total electron collision frequency (electron-neutral + electron - ion) 41

LIST OF SYMBOLS

a	speed of sound
C_D	drag coefficient
f	velocity ratio defined in Eq. (6)
H	altitude
h	enthalpy
M	Mach number
N_e	electron density
p	pressure
R	Howarth radius defined in Eq. (4) or gas constant
r	radial distance from axis
r_o	radius of body
S	entropy
T	temperature
U	velocity in axial direction
V	velocity with respect to stationary atmosphere
W	body weight
X	normalized axial distance defined in Eq. (10)
x	axial distance
z	compressiblity factor $z = \frac{pV}{RT}$
γ	ratio of specific heats C_p/C_v
μ	viscosity
ν_e	collision frequency of electrons with ions and neutrals
ρ	density

SUBSCRIPTS

o	standard conditions
∞	free stream
p	station at which $p = p_\infty$

I. INTRODUCTION

Recently there has been a great deal of interest in the problem of absorption and reflection of electromagnetic energy from the ionized trail or wake left by a body moving at hypersonic velocities. In order to determine the electromagnetic properties of the wake, it is necessary to know in some detail the structure of the wake in terms of the important electromagnetic parameters such as electron density, collision frequency, velocity, temperature, etc.

The structure of the wake has been investigated by many authors. Using numerical techniques, Feldman[1,2] was one of the first to examine the wake structure. Recently, Lykoudis[3] has investigated the problem using an analytic approach throughout. Any of the above references will provide the reader with an excellent introduction to the fundamental nature of the wake. It is the purpose of this note to transform the analytic results of Lykoudis,[3] which are in terms of the enthalpy, into the above electromagnetic parameters. At the same time an attempt will be made to collect and reorganize the necessary collateral data.

In Section II a brief general discussion of the wake will be given. Section II will introduce the following sections, and will discuss the basic assumptions and limitations of the model. In Section III, Lykoudis' results for the conduction-controlled part of the wake are presented, and in Section IV we provide the necessary data for translating the Lykoudis model into the important electromagnetic parameters, and an approximate analytic model for the electromagnetic properties is derived.

II. GENERAL DISCUSSION OF THE WAKE

The structure of the hypersonic wake behind a blunt body is shown in Fig. 1. For a detailed discussion of the structure the reader is referred to Ref. 3. Referring to Fig. 1, we may briefly describe the flow pattern as follows. The free-stream air is irreversibly compressed while passing through the bow shock. The air then expands and is recompressed in the trailing shock. This is followed by further expansion and at some station ($x = x_p$) the air has expanded to the free stream pressure p_∞.

The portion of the flow which enters the boundary layer forms the viscous wake. Beyond the station $x = x_p$ the wake is characterized by the diffusion of energy out of the central viscous part of the wake. In a laminar wake this transport takes place by molecular diffusion; in a turbulent wake the process takes place by turbulent diffusion and mixing.

Our discussion will be restricted to blunt bodies. For slender bodies the shock is weaker and the viscous wake contains most of the momentum loss and high-temperature air. As a result the electromagnetic parameters depend critically on the boundary layer at the trailing edge of the body, and hence on the afterbody shape. For blunt bodies it has been shown that the exact shape of the afterbody does not appreciably affect the nature of the wake. This occurs because the inviscid flow, which is relatively unaffected by the afterbody and trailing shock, contains most of the momentum defect by means of the strong bow shock, and hence the bow shock controls the behavior of the wake in this case. We shall assume that this is the

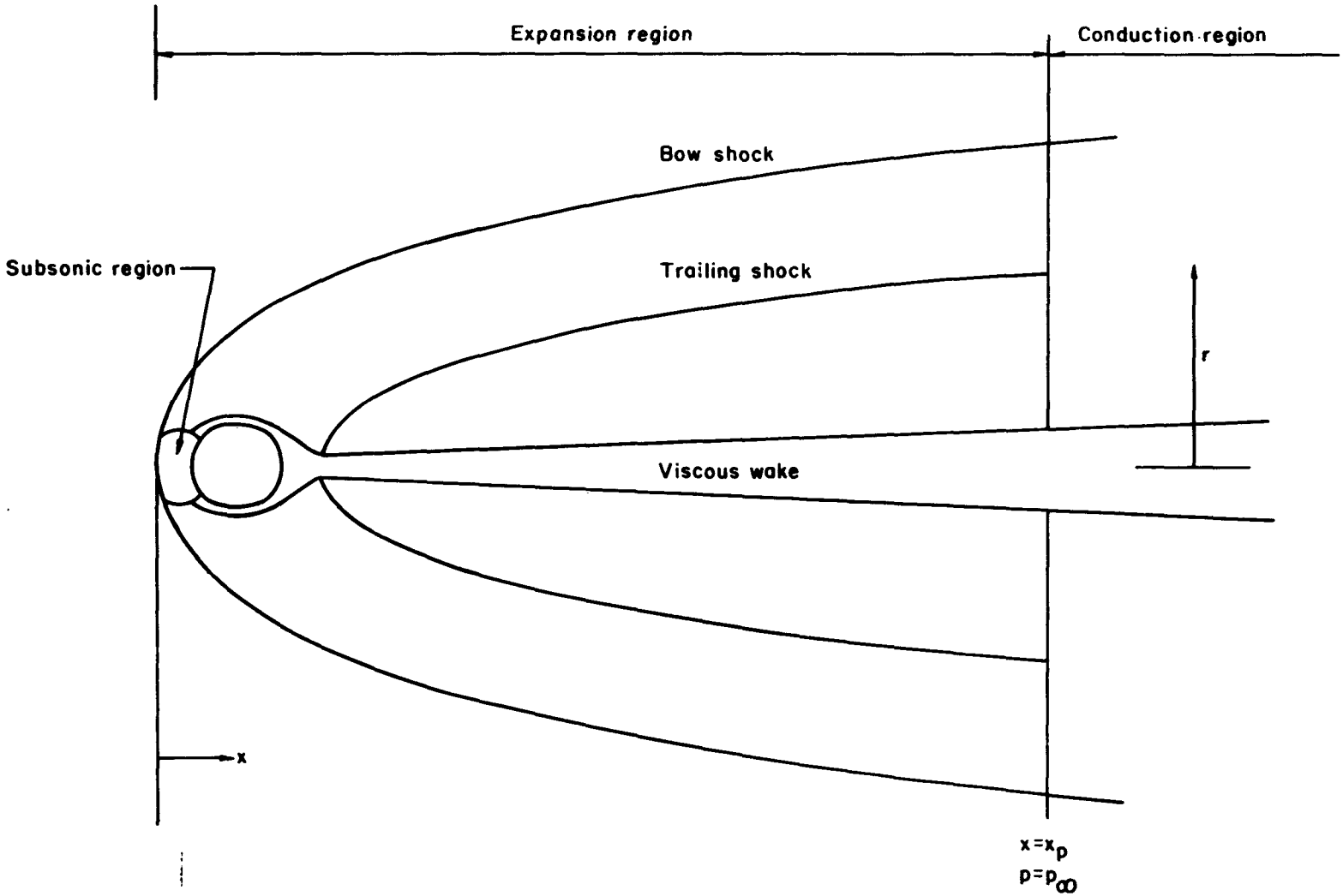

Fig. 1— Structure of the hypersonic wake

case and thus we shall ignore the contribution of the trailing shock to the pressure and the velocity. Neglecting the afterbody and neck shock is equivalent to assuming that the wake may be computed from the nature of the bow shock alone.

We shall also neglect the effects of the boundary layer contributions to the viscous wake and consider instead that the far laminar wake is a gas cylinder with a given initial temperature distribution which cools by conduction and convection. This assumption is tantamount to the neglect of turbulence, where the principal radial cooling mechanism is turbulent diffusion. It appears that this assumption is reasonable for a significant range of flight conditions, in particular for blunt bodies at altitudes above 180,000 ft and below 250,000 ft. At altitudes above 250,000 ft we violate our assumption that the flow is inviscid; and at altitudes below about 180,000 ft the flow is likely to be turbulent, and thus we violate our assumption that the flow is laminar. A detailed discussion of the structure of the turbulent wake will be found in Ref. 4.

The effects of turbulence on the electromagnetic properties of the wake are two-fold. First, turbulence tends to cool the wake much more rapidly, and second, turbulence introduces local fluctuations in the parameters. This complicates the scattering problem by aerodynamically "roughening" the surface of the wake. This causes interference of the incoming and reflected electromagnetic waves, and in general, significantly changes the amplitude of the scattered energy. The magnitude of the turbulent effect is, of course, a function of the scale of the turbulence as well as the radar frequency and mean electron density.

The normal procedure for analyzing a wake is to divide the wake into two distinct regions, one of which is controlled by expansion of the inviscid flow, and the other determined by an energy balance of axial convection and radial conduction from the inner wake. The expansion region starts (when the neck shock is neglected) at the bow wave and continues until the diffusive or molecular processes become important, somewhere in the vicinity where the pressure approaches ambient values. For convenience, we will assume that the expansion region includes all the flow from the bow shock up the point $x = x_p$ where $p = p_\infty$. In this region the flow is assumed to be inviscid and adiabatic.

The second region is called the conduction region and is the remainder of the wake. In this region the only important mechanism is assumed to be the cooling of the wake by thermal conduction.

In some cases a significant amount of conduction cooling takes place before the pressure reaches ambient values, at station x_p. For our two-region model to be valid, this conduction cooling must be small compared to the exapnsion process. A detailed study of the relative magnitudes of these two processes has been made by Lykoudis.[5] His results indicate that for body radii greater than r_{min}, where

$$r_{min} = \frac{5M^2 \mu_\infty}{\rho_\infty U_\infty} \tag{1}$$

the two-region model is adequate.

For typical re-entry conditions the Reynolds number is high and Eq. (1) indicates that our two-region model would be adequate for bodies larger than 1 cm in radius.

For altitudes above 200,000 ft the flow may be considered "frozen" for bodies which have a nose radius of 1 ft or greater, and the composition of the wake air may be considered to be the same as the composition of equilibrium air under stagnation conditions. On the other hand, for altitudes below 100,000 ft the relaxation rates are sufficiently fast so that the air may be considered to be in thermodynamic equilibrium with the local conditions. In order to simplify the calculations we shall assume that the air is in thermodynamic equilibrium with the local conditions at all times.

The effect of ablation products on the electron density and other electromagnetic parameters can be very important. With some reluctance we will neglect the ablation products in our analysis. There are two reasons for this. First, very little information is available on the equilibrium characteristics of air containing typical concentrations of ablation products and second, since we have neglected the boundary layer there is no appropriate way to introduce the ablation products into the problem.

In Ref. 3, it is pointed out that the length of the expansion region is small compared to the length of the conduction region. The length of the expansion region may be estimated from

$$x_p \simeq \frac{r_o M^2}{4.5} \tag{2}$$

Since the expansion region is small we will consider only the conduction part of the wake. If the reader wishes to include the expansion region in his model he may use the results presented in Ref. 3.

In the next section we will present Lykoudis' results for the conduction region.

III. SIMPLIFIED MODEL OF THE CONDUCTION REGION OF THE WAKE

In this section we present Lykoudis' universal solution for the enthalpy in the conduction region. The first part of this solution determines the enthalpy profile at the station $x = x_p$. Lykoudis obtained the following result from the conservation of total enthalpy

$$\frac{h(x_p,r)}{h(x_p,o)} = \frac{1}{\left(1 + \frac{4 f R^2}{a C_D r_o^2}\right)^{1/\gamma_2}} \tag{3}$$

where we have introduced the Howarth radius R which is related to the actual radius r by

$$r^2 = \int_o^R \frac{\rho_\infty}{\rho(R)} 2RdR \tag{4}$$

The term γ_2 is an effective ratio of specific heats which is approximately 1.2 for hypervelocity flight conditions. The parameter a and the drag coefficient C_D determine the shape of the bow shock. Reference 4 gives the following relation for the bow shock

$$R = (a\ C_D)^{1/4} \sqrt{\frac{x}{r_o}} \tag{5}$$

a is approximately 2.6 and f is defined below:

$$f = \frac{U_{x_p}}{U_\infty} \cong \sqrt{1 - \frac{1}{M^{1/3}}} \tag{6}$$

f varies between 0.77 and 0.83 as M varies between 15 and 35.

Feldman[1,2] has numerically computed the enthalpy profile at $x = x_p$ by using the method of characteristics. Lykoudis[3] makes a comparison between Feldman's results and Eq. (3). The two results agree very well. Lykoudis[3] and Feldman[1,2] have also compared a gaussian profile (to be considered later) with Feldman's results. The gaussian profile agrees with Feldman's results for small R, but diverges for $R > r_o$, where Eq. (3) becomes a better approximation.

We note that Eq. (3) may be approximated by

$$\frac{h(x_p,r)}{h(x_p,o)} \cong \frac{1}{1 + \frac{R^2}{C_D\, r_o^2}} \tag{7}$$

A solution for the enthalpy in the conduction region may be found (assuming constant thermal conductivity) for the boundary condition given in Eq. (3). This solution is given in terms of a complicated Fourier-Bessel integral. In order to simplify the problem, let us assume, following Feldman[1,2] and Lykoudis,[3] that the initial distribution at $x = x_p$ is gaussian.

$$\frac{h(x_p,r)}{h(x_p,o)} = e^{-\frac{R^2}{C_D\, r_o^2}} \tag{8}$$

Neither Eq. (3) nor Eq. (8) are valid for $R \geq R_s$, where R_s is the

radius of the bow shock at $x = x_p$. For $R \geq R_S$ the enthalpy is, of course, equal to the ambient enthalpy, h_∞.

A comparison of Eq. (8) with Eq. (7) indicates that the two distributions match very well for small R, and as long as we restrict our solutions to small R no serious errors will arise.

The use of Eq. (8) has the advantage that the energy equation in the conduction region can be solved in closed form even when the thermal conductivity is variable. It can be shown from Ref. (3) that the enthalpy distribution for regions downstream of $x = x_p$ is given by

$$\frac{h(x,r)}{h(x_p,o)} = \frac{e^{-\frac{R^2}{(1+X)^{0.8}\, C_D\, r_o^2}}}{(1+X)^{0.8}} \tag{9}$$

where

$$X = \frac{\left(\frac{h(x_p,o)}{R\,T_o}\right)^{1/4}}{0.5345\,\frac{\rho_\infty}{\rho_o}\,U_\infty}\;\frac{(x - x_p)}{C_D\; r_o^2}$$

in cgs units.

Now for small R we can replace the exponential in Eq. (9) by:

$$e^{-\frac{R^2}{(1+X)^{0.8}\, C_D\, r_o^2}} \cong \frac{1}{1 + \frac{R^2}{(1+X)^{0.8}\, C_D\, r_o^2}} \tag{10}$$

Therefore Eq. (9) may be written as

$$\frac{h(x,r)}{h(x_p,o)} = \frac{1}{(1 + X)^{0.8} + \frac{R^2}{C_D\, r_o^2}} \tag{11}$$

We note in passing that the substitution we have just made is not likely to introduce additional errors into our computation, but to the contrary it is likely to improve our answer since Eq. (11) satisfies the more accurate boundary condition Eq. (7).

We summarize our universal solution as follows:

$$\frac{h(x,r)}{R\, T_o} = \frac{h(x_p,o)}{R\, T_o \left[(1 + X)^{0.8} + \frac{R^2}{C_D\, r_o^2}\right]} \tag{12}$$

$$X = \frac{\left(\frac{h(x_p,o)}{R\, T_o}\right)^{1/4}}{0.5345\, \frac{\rho_\infty}{\rho_o}\, U_\infty} \; \frac{(x - x_p)}{C_D\, r_o^2} \tag{13}$$

$$r^2 = \int_o^R \frac{\rho_\infty}{\rho(R)}\, 2R dR \tag{14}$$

In the next section we will discuss the numerical computation of h and its translation into the electromagnetic parameters.

IV. DETERMINATION OF THE WAKE PROPERTIES FROM THE SIMPLIFIED MODEL

In this section we will provide the data for determining the parameter profiles for a given set of re-entry conditions. We assume that the vehicle velocity (free stream velocity U_∞), the altitude H, the drag coefficient C_D, and the body radius r_o are given. The terms U_∞ and H are taken from the trajectory of the body; examples are shown in Fig. 2.

The first step is to translate our altitude data into the required ambient or free stream thermodynamic parameters. To do this we will assume the ARDC model atmosphere.[6] The thermodynamic variables are plotted as a function of altitude in Figs. 7 through 12 in Appendix A. For simplicity we will assume the ambient conditions do not change appreciably over that portion of the wake in which we are interested, and thus may be taken as constant. The range of ambient conditions should be checked and an appropriate average value chosen. If a more accurate solution is desired, the wake may be divided up into a number of sections where the ambient conditions of each section may be considered constant.

Our next step will be to compute $h(x,r)/RT_o$ from Eqs. (12), (13), and (14). The only quantity appearing in these expressions which cannot be read directly from Figs. 7 through 12 is $h(x_p,o)/RT_o$. This quantity may be computed from shock tables[7] or from the approximate relation below, which is derived in Ref. 4 from the energy equation assuming that $f = 0.3$.

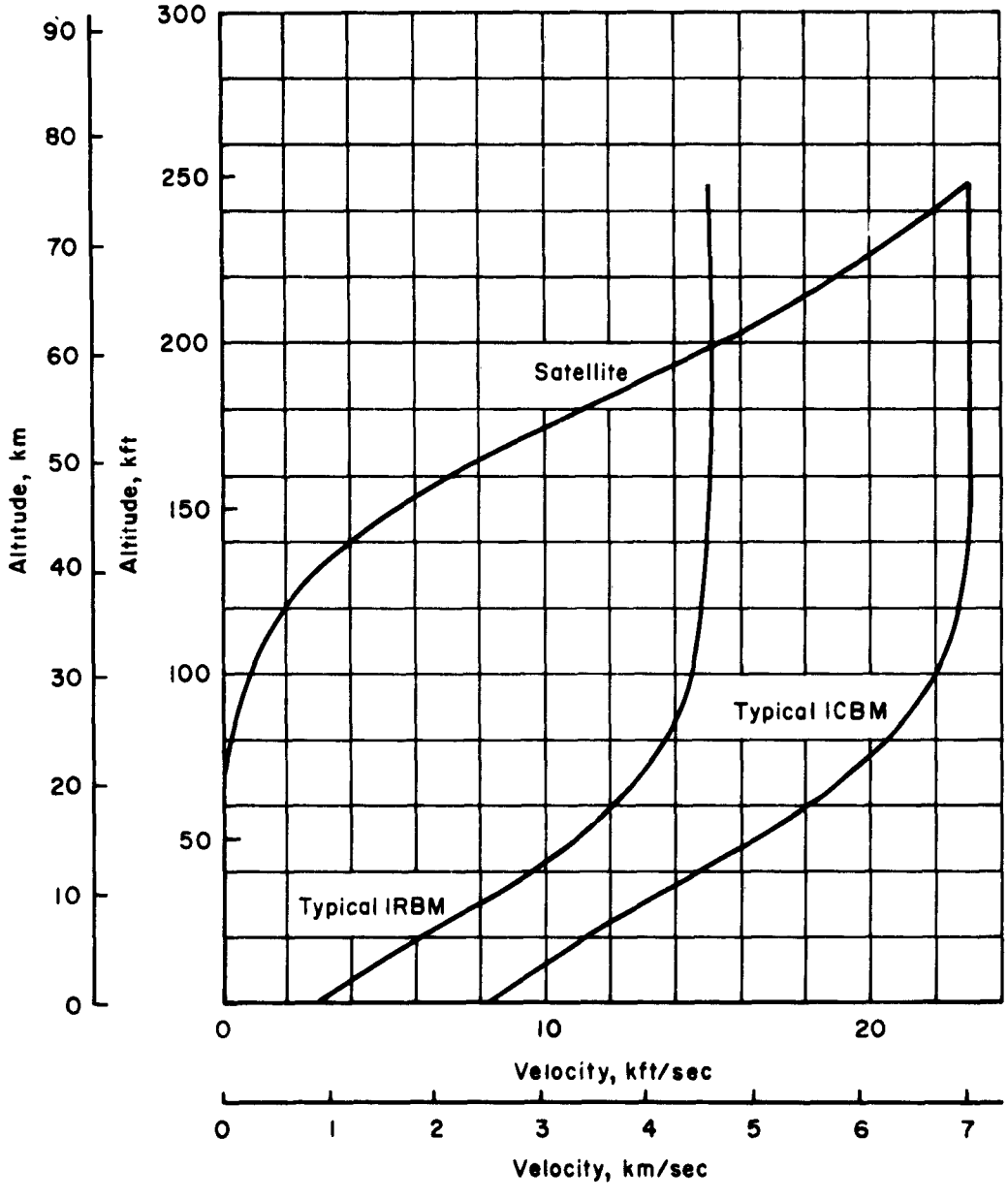

Fig. 2—Typical re-entry trajectories

$$\frac{h(x_p,o)}{R\,T_o} \cong \frac{h_\infty}{R\,T_o}\;\frac{(\gamma - 1)\,M^2}{6} \tag{15}$$

where $M = \frac{U_\infty}{a_\infty}$. The term $h(x,r)/RT_o$ is now completely determined.

We next turn to the problem of determining the thermodynamic and electromagnetic parameters from $\frac{h}{R\,T_o}$ for a given pressure $\frac{p_\infty}{p_o}$ (i.e., altitude). First let us consider the average velocity of the air in the wake. For a constant stagnation enthalpy in the radial direction (Prandtl number unity) the conservation of energy implies that

$$1 - \left[\frac{U(x,r)}{U_\infty}\right]^2 = \frac{2h_\infty}{U_\infty^2}\left[\frac{h(x,r)}{h_\infty} - 1\right] \tag{16}$$

For $h/h_\infty \gg 1$ and $U/U_\infty \ll 1$ the above expression reduces to

$$1 - \frac{U(x,r)}{U_\infty} \simeq 2\,\frac{h(x,r)}{h_\infty}\cdot\frac{h_\infty}{U_\infty^2}$$

which can be compared with its value at $x = x_p$, $r = 0$ to yield

$$1 - \frac{U(x,r)}{U_\infty} = \left[1 - \frac{U(x_p,o)}{U_\infty}\right]\frac{h(x,r)}{h(x_p,o)} \tag{17}$$

We recall that

$$\frac{U(x_p,o)}{U_\infty} = f \approx 0.8 \tag{18}$$

so therefore the air velocity with respect to a stationary atmosphere is given by

$$V = U_\infty - U(x,r) = 0.2\, U_\infty \frac{h(x,r)}{h(x_p,o)} \tag{19}$$

The remaining parameters are presented graphically as a function of h/RT_o for various values of $\log \frac{p_\infty}{p_o}$ under the assumption that the air is locally in equilbrium. The S, ρ, T and z curves were obtained from Blackwell,[8] the N_e curves from Gilmore,[9] and the ν_e curves from Romig.* These curves are shown in Figs. 13 through 19, in Appendix B.

In some applications one prefers to have the structure of the wake presented in graphical form; for example electron density contours. In this case, the most efficient way to obtain the graphical representation is simply to plot it point-by-point from the graphs presented in Appendix B. However, in most applications the structure of the wake serves as a starting point for the analysis of a particular problem; for example, the computation of the radar cross section. In this case it is much more convenient to have the structure of the wake presented in analytic form. In this section we will illustrate the technique of determining an approximate analytic representation by considering a specific example.

*Private communication.

The input conditions for the specific case to be considered are given below:

$$U_\infty = 25{,}000 \text{ ft/sec} = 7.62 \times 10^5 \text{ cm/sec} \tag{20}$$

$$H = 100{,}000 \text{ ft} \tag{21}$$

The terms C_D and r_o will be retained as parameters and r_o is to be given in centimeters. This altitude was selected so that the results could be compared with Feldman, however the wake is likely to be turbulent at this altitude.

Using these input conditions we readily obtain the following results:

From Fig. 7 $$\frac{h_\infty}{R\,T_o} = 2.78 \tag{22}$$

From Fig. 8 $$\frac{\rho_\infty}{\rho_o} = 1.28 \times 10^{-2} \tag{23}$$

From Fig. 10 $$\log \frac{p_\infty}{p_o} = -1.96 \tag{24}$$

From Fig. 11 $$a_\infty = 994 \text{ ft/sec} \tag{25}$$

Therefore $$M = 25.2 \tag{26}$$

From Eq. (15) $$\frac{h(x_p,o)}{R\,T_o} = 117 \tag{27}$$

From shock tables $$\frac{h(x_p,o)}{R\,T_o} = 142 \tag{28}$$

We shall use the value obtained from the shock tables, since Eq. (15) gives only an approximate value for h. For this particular case Eq. (15) gives a value which is about 15 per cent below the correct value.

From Eq. (13) $$X = 6.64 \times 10^{-4} \frac{(x - x_p)}{C_D\, r_o^2} \tag{29}$$

From Eq. (2) $$x_p \simeq 140\, r_o \tag{30}$$

From Eq. (12) $$\frac{h(x,r)}{R\,T_o} = \frac{142}{(1 + X)^{0.8} + \dfrac{R^2}{C_D\, r_o^2}} \tag{31}$$

Since we will only be interested in the structure of the wake where $\frac{h}{R\,T_o} \geq 30$, or for electron densities greater than 10^6 electrons/cm^3, the overall range of $\frac{h}{R\,T_o}$ to be considered is

$$30 \leq \frac{h}{R\,T_o} \leq 150 \tag{32}$$

Next we will determine the density as a function of $\frac{h}{R\ T_o}$. This relation is given graphically in Fig. 14. The density curve can be approximated by a straight line to within a factor of 1.1 for the range of values given in Eq. (32). The straight line on log-log paper gives the following power law relation:

$$\frac{\rho}{\rho_o} = 10^{-2} \left(\frac{h}{R\ T_o}\right)^{-0.6} \tag{33}$$

or

$$\frac{\rho}{\rho_\infty} = 0.78 \left(\frac{h}{R\ T_o}\right)^{-0.6} \tag{34}$$

From Eq. (14)

$$r^2 = \int_o^R \frac{2R\ dR}{0.78 \left[\dfrac{142}{(1 + X)^{0.8} + \dfrac{R^2}{C_D\ r_o^2}}\right]^{-0.6}} \tag{35}$$

Integrating Eq. (35) gives

$$(1 + X)^{0.8} + \frac{R^2}{C_D\ r_o^2} = \left[(1 + X)^{0.32} + 0.016\ \frac{r^2}{C_D\ r_o^2}\right]^{2.5} \tag{36}$$

Substituting Eqs. (29) and (36) into Eq. (31) gives

$$\frac{h(x,r)}{R\,T_o} = \frac{142}{\left[\left(1 + 6.64 \times 10^{-4} \frac{[x - x_p]}{C_D\, r_o^2}\right)^{0.32} + 0.016 \frac{r^2}{C_D\, r_o^2}\right]^{2.5}} \tag{37}$$

The other quantities may be determined as a function of $\frac{h}{R\,T_o}$ by empirically fitting the appropriate curve for the given range of $\frac{h}{R\,T_o}$. Since the other quantities depend only on the enthalpy, the constant enthalpy contours may be interpreted as contours of the other quantities also.

Let us consider the electron density relation as an illustrative example of the technique. The electron density relation is shown in Fig. 18. The curve may be fitted to within a factor of 5 by a straight line for the given range of $\frac{h}{R\,T_o}$.

$$N_e = 2 \times 10^{-8} \left(\frac{h}{R\,T_o}\right)^{9.3} \quad \frac{\text{electrons}}{\text{cm}^3} \tag{38}$$

Substituting Eq. (37) into (38) gives

$$N_e = \frac{2 \times 10^{12}}{\left[\left(1 + 6.64 \times 10^{-4} \frac{[x - x_p]}{C_D\, r_o^2}\right)^{0.32} + 0.016 \frac{r^2}{C_D\, r_o^2}\right]^{23.2}} \quad \frac{\text{electrons}}{\text{cm}^3} \tag{39}$$

The other quantities such as temperature, collision frequency, etc., may be found in a similar fashion.

For other re-entry conditions one obtains expressions for the electron density which are very similar in form to Eq. (39). For example, H = 100,000 ft and U_∞ = 20,000 ft/sec gives

$$N_e = \frac{2.4 \times 10^{10}}{\left[\left(1 + 7.21 \times 10^{-4} \frac{[x - x_p]}{C_D r_o^2}\right)^{0.32} + 0.021 \frac{r^2}{C_D r_o^2}\right]^{23.2}} \tag{40}$$

In Figs. 3 and 4 we compare Eqs. (39) and (40) with the numerical results of Feldman.[2] Figure 3 shows the radial variation in the electron density at $x = x_p$ and Fig. 4 shows the axial variation in the electron density for r = o.

Figure 3 indicates that the results are in close agreement for small r, but tend to diverge for large r. This divergence may be traced to the assumption given in Eq. (10). Feldman retains the exponential form corresponding to the left-hand side of Eq. (10), while we prefer to use the inverse form corresponding to the right-hand side of Eq. (10). Since the exponential form falls off more rapidly with increasing r than the inverse form does, the simplified model will tend to give a somewhat broader wake.

Figure 4 indicates that there is a basic difference between Lykoudis' and Feldman's expressions for the enthalpy as a function of x. In terms of electron density the two solutions differ by a factor of about 10, however, this corresponds to only a small 10 per cent

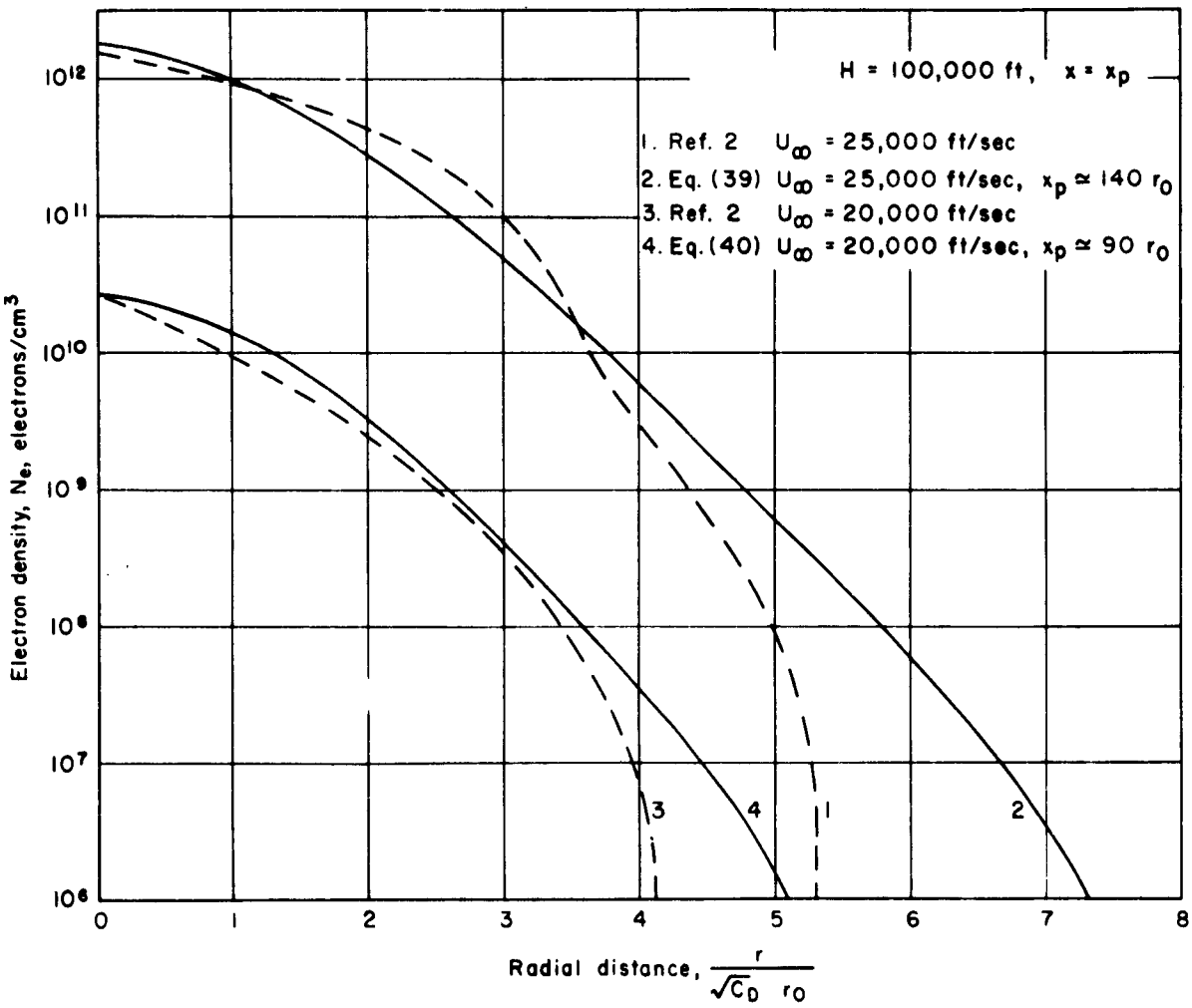

Fig. 3 — Radial electron distribution

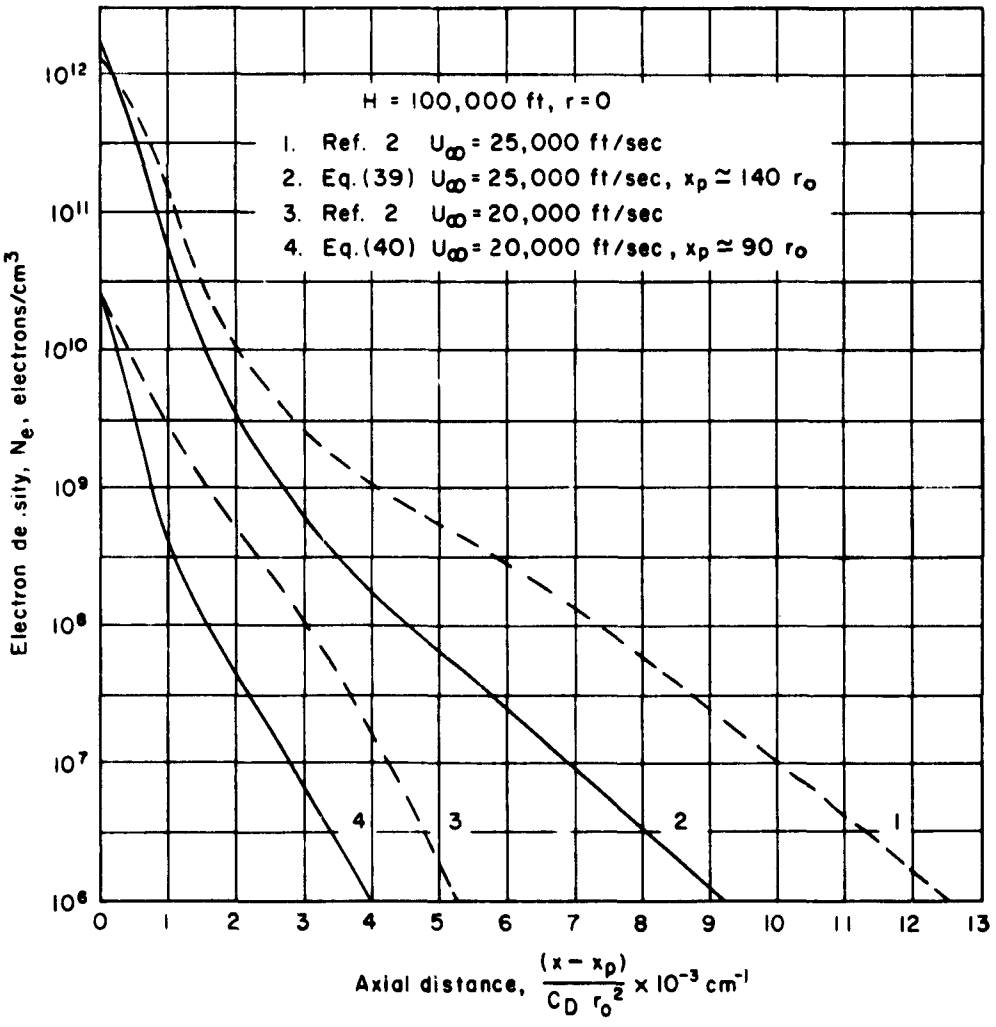

Fig. 4 —Axial electron distribution

difference in terms of enthalpy. Thus in terms of enthalpy the two solutions are almost the same. Indeed, it appears that the uncertainties introduced by the simplifying assumptions which have been made in both analyses will overshadow the discrepancies between the two results.

The two results are in very close agreement for the "hot" portion of the wake (i.e., small r, small x). The "hot" portion is often the region of most interest. In the outside or cooler part of the wake the simplified model gives solutions for the wake which are somewhat broader and shorter than the solutions given by Feldman.

Finally, the nature of the wake is shown in Figs. 5 and 6. Figure 5 is a plot of Eq. (39) and Fig. 6 is a plot of Eq. (40). The axial distance is, of course, greatly compressed in comparison with the radial distance. For a one meter body the trail is about 5×10^4 longer than it is wide.

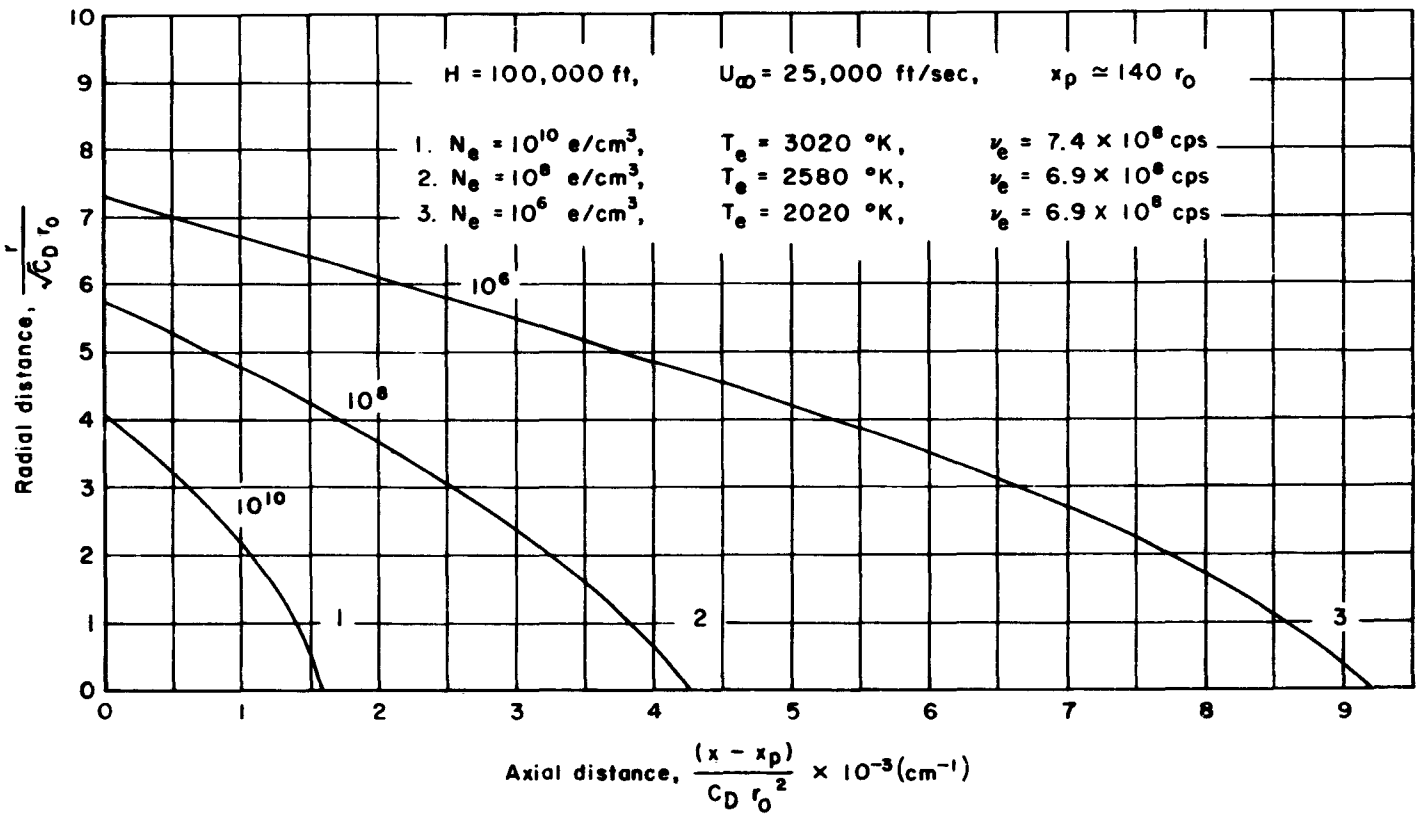

Fig. 5 — Electron density profiles (Case I)

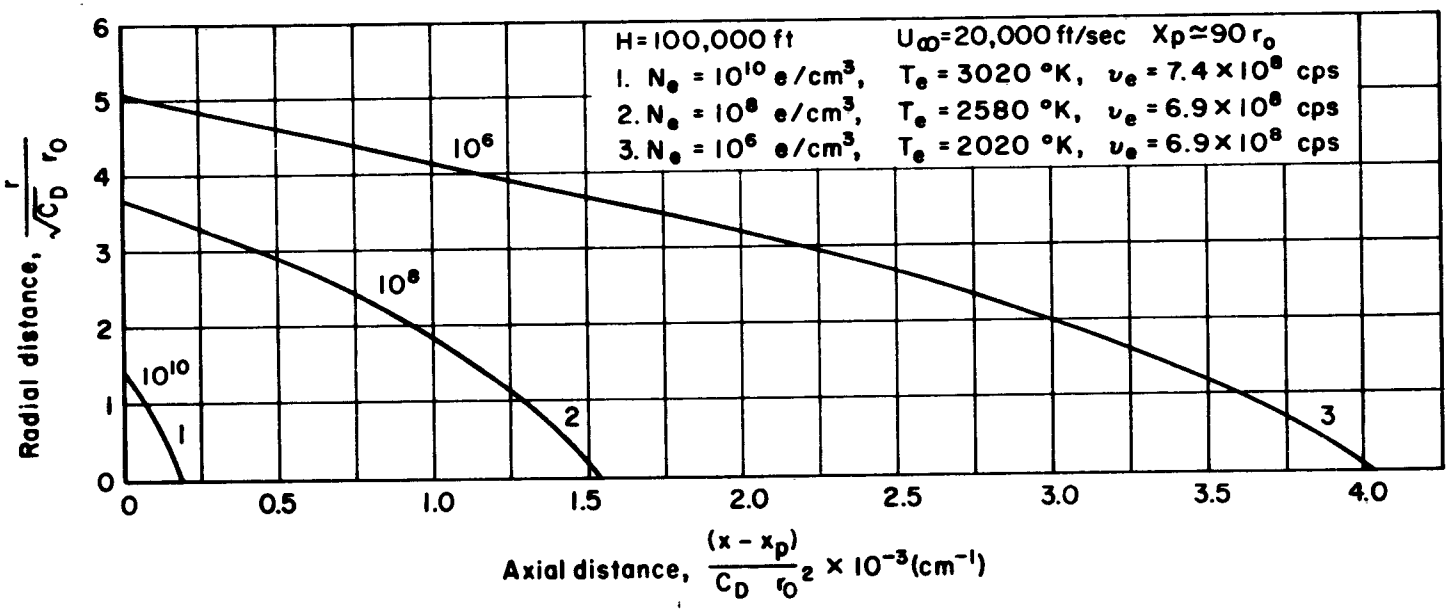

Fig. 6 — Electron density profiles (Case 2)

V. CONCLUSIONS

The simplified model discussed in this paper is applicable to that portion of the re-entry trajectory where the flow may be considered to be inviscid and laminar. This corresponds roughly to a range of altitudes from 180,000 to 250,000 ft. The viscous effects become important above 250,000 ft and the flow is likely to be turbulent below 180,000 ft. In this range of altitudes the model gives results which agree with the numerical results of Feldman.[2]

In computing the electromagnetic characteristics of the wake, the air was assumed to be in equilibrium with the local conditions. This assumption is not valid for altitudes much higher than 100,000 ft. Assuming local equilibrium at altitudes above 100,000 ft will provide a lower limit for the actual electron density. At altitudes above 200,000 ft we may assume the flow to be "frozen," and thus compute the electromagnetic characteristics from the stagnation conditions. For the intermediate or transitional altitudes the two limiting cases will serve as upper and lower bounds for the solution.

Appendix A

(Figures 7-12)

ARDC MODEL ATMOSPHERE[6]

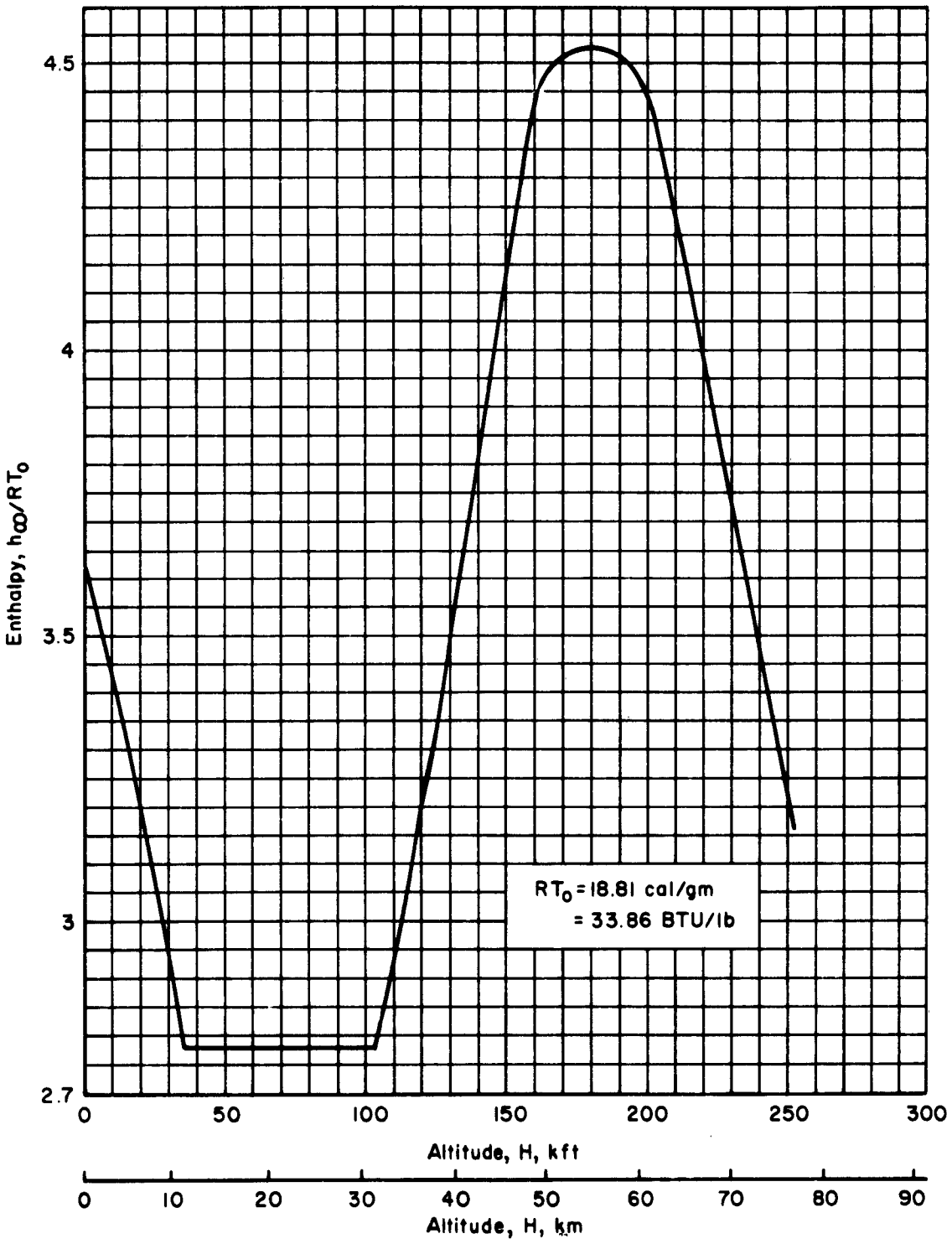

Fig. 7 — Enthalpy

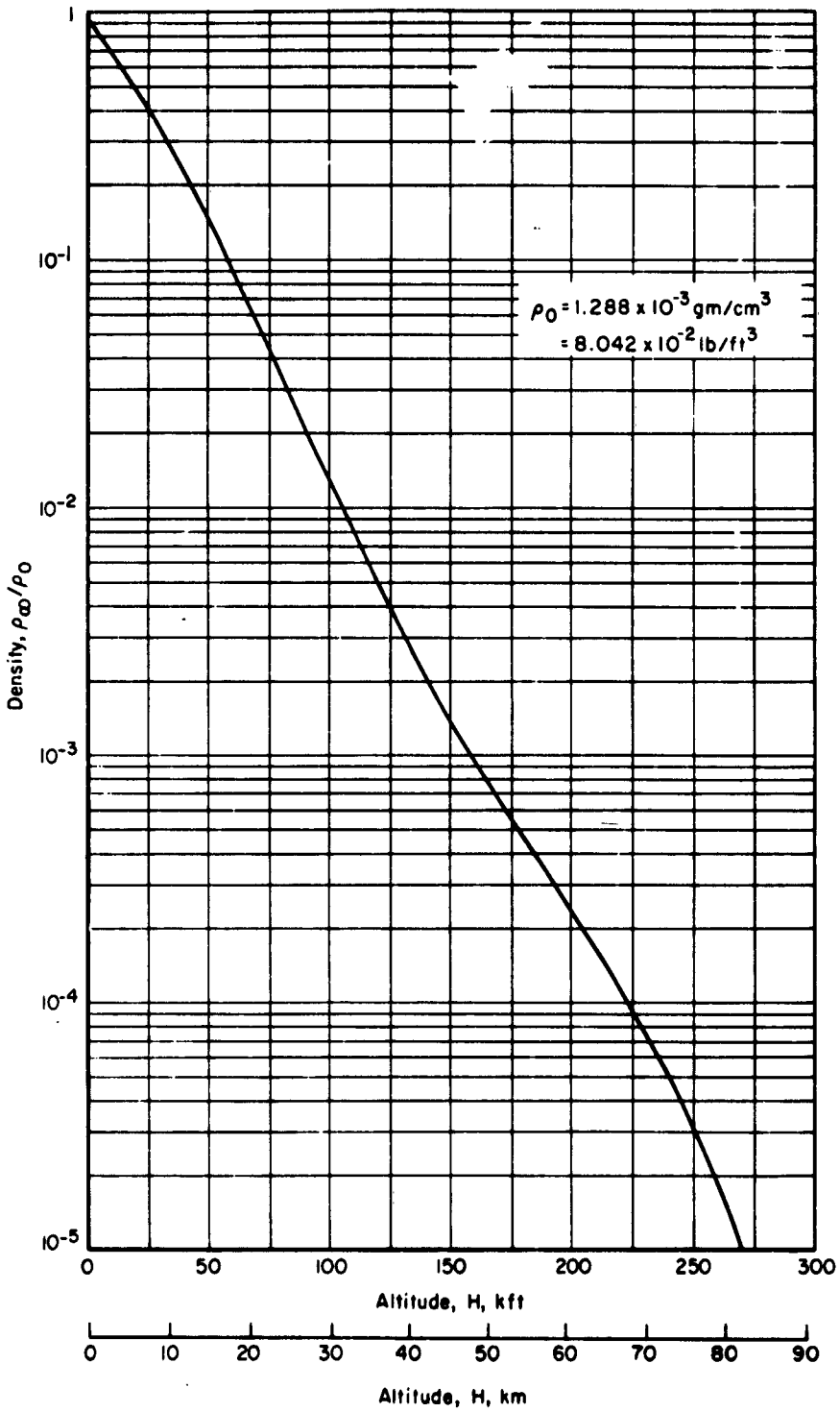

Fig. 8 — Density

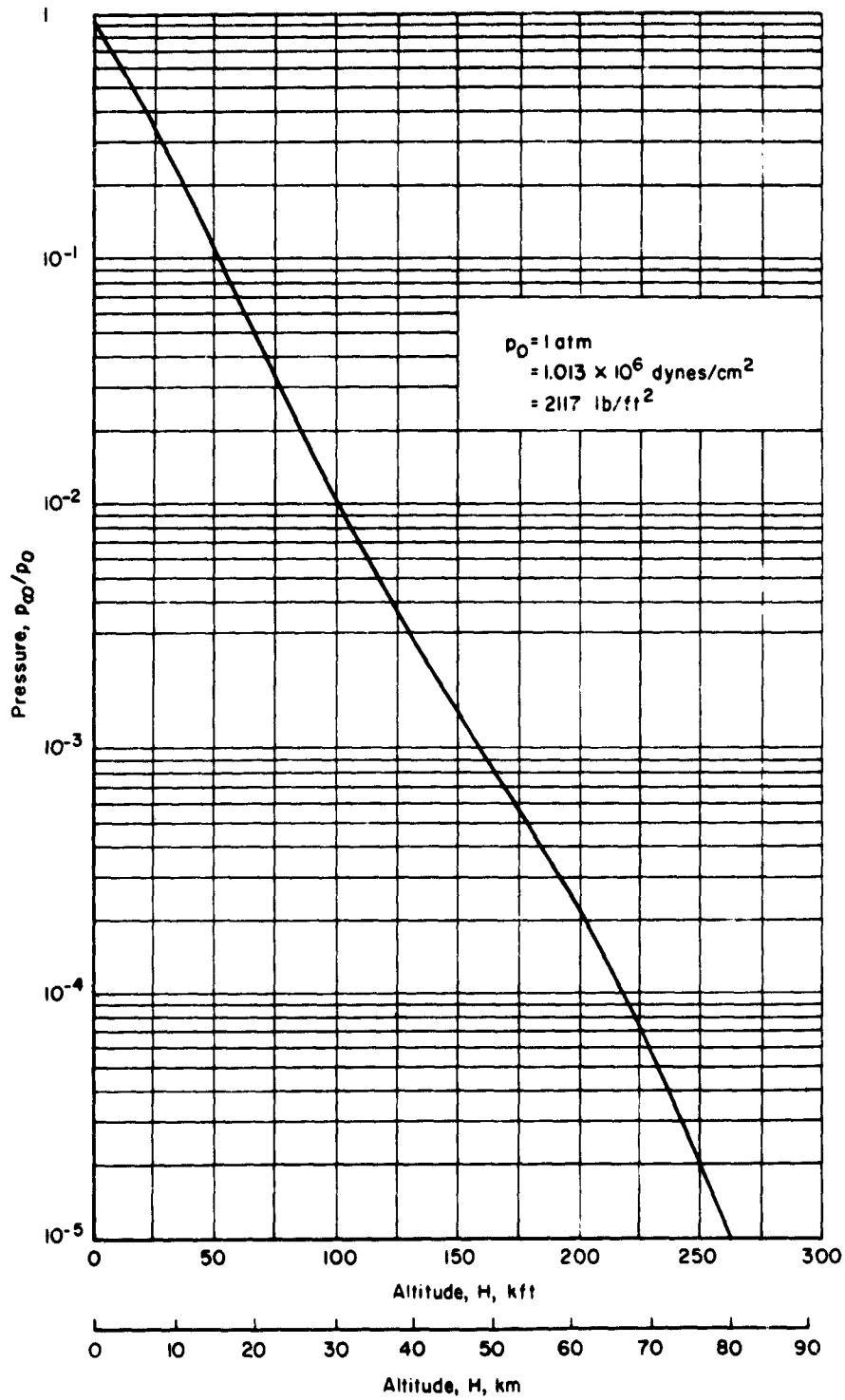

Fig. 9 — Pressure

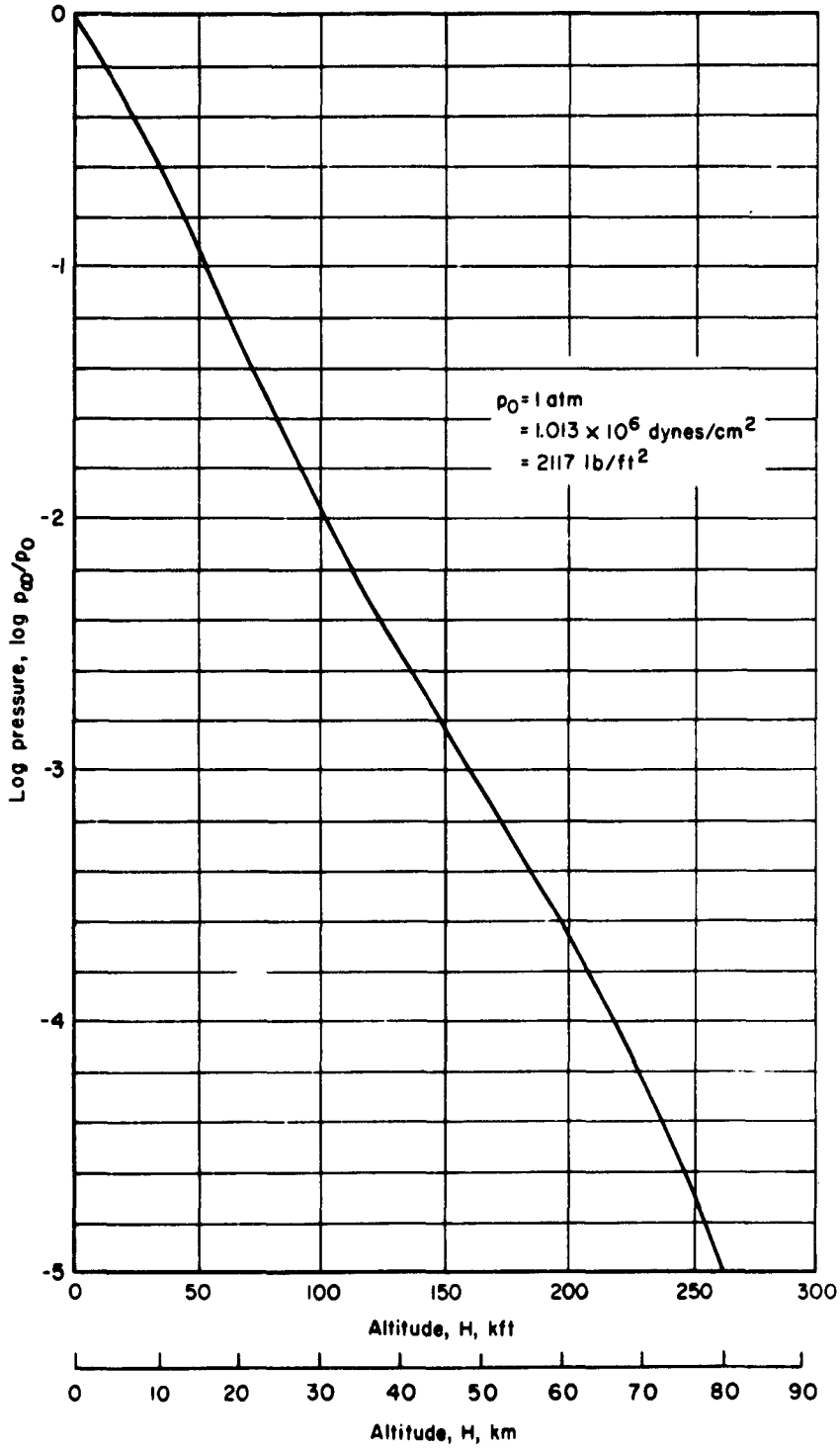

Fig. 10 — Log pressures

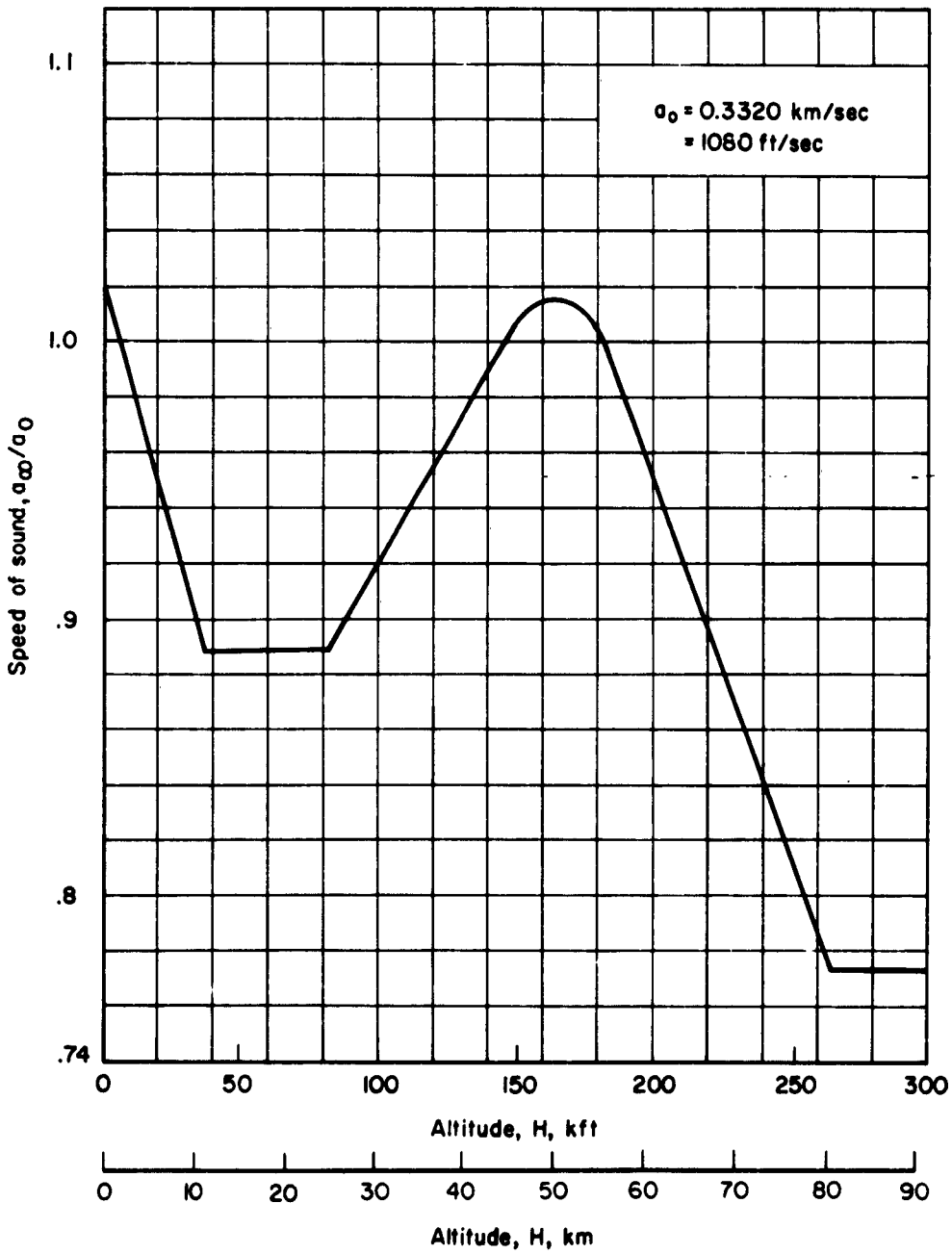

Fig. 11—Speed of sound

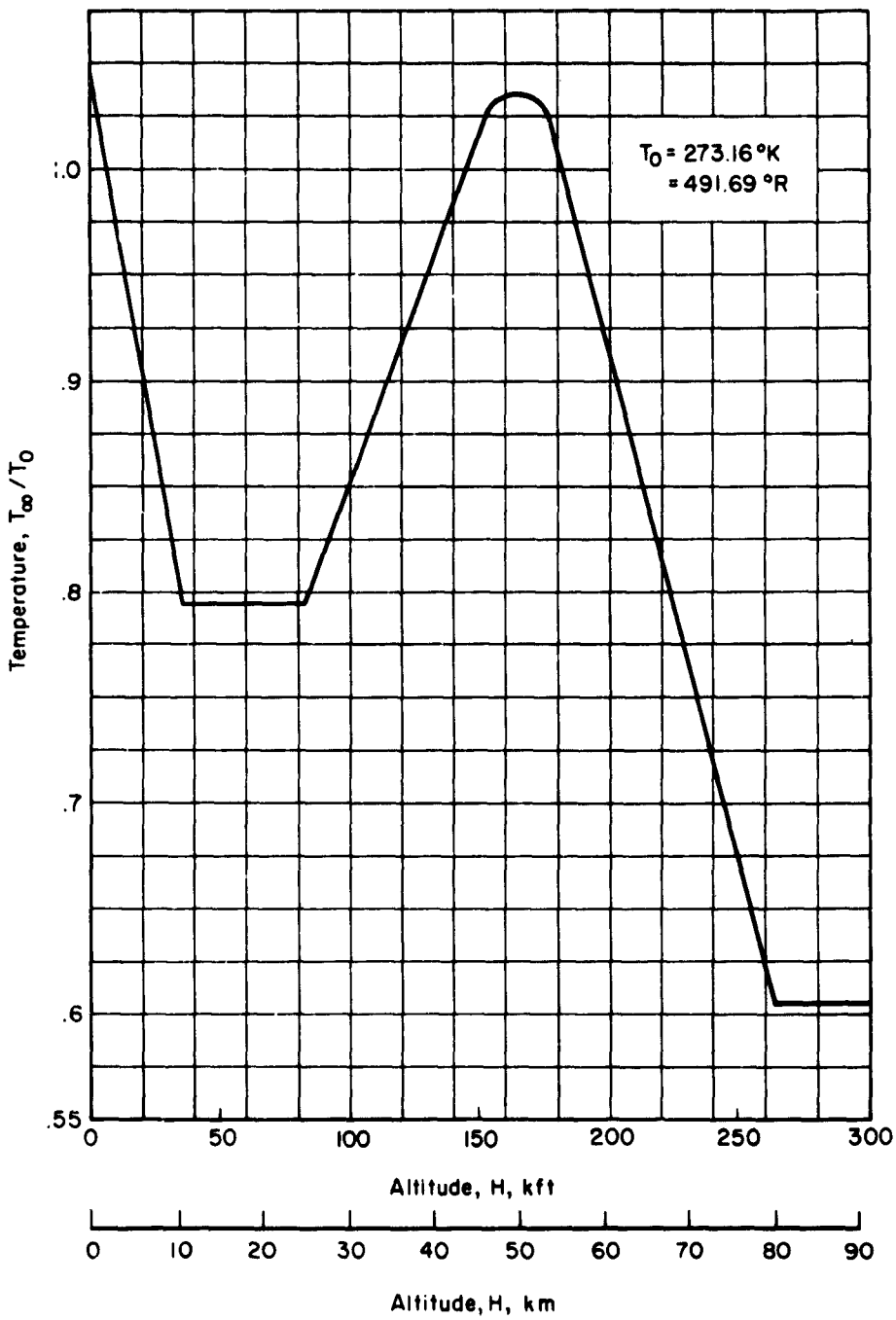

Fig. 12 — Temperature

Appendix B

(Figures 13-19)

PROPERTIES OF EQUILIBRIUM AIR[8,9]

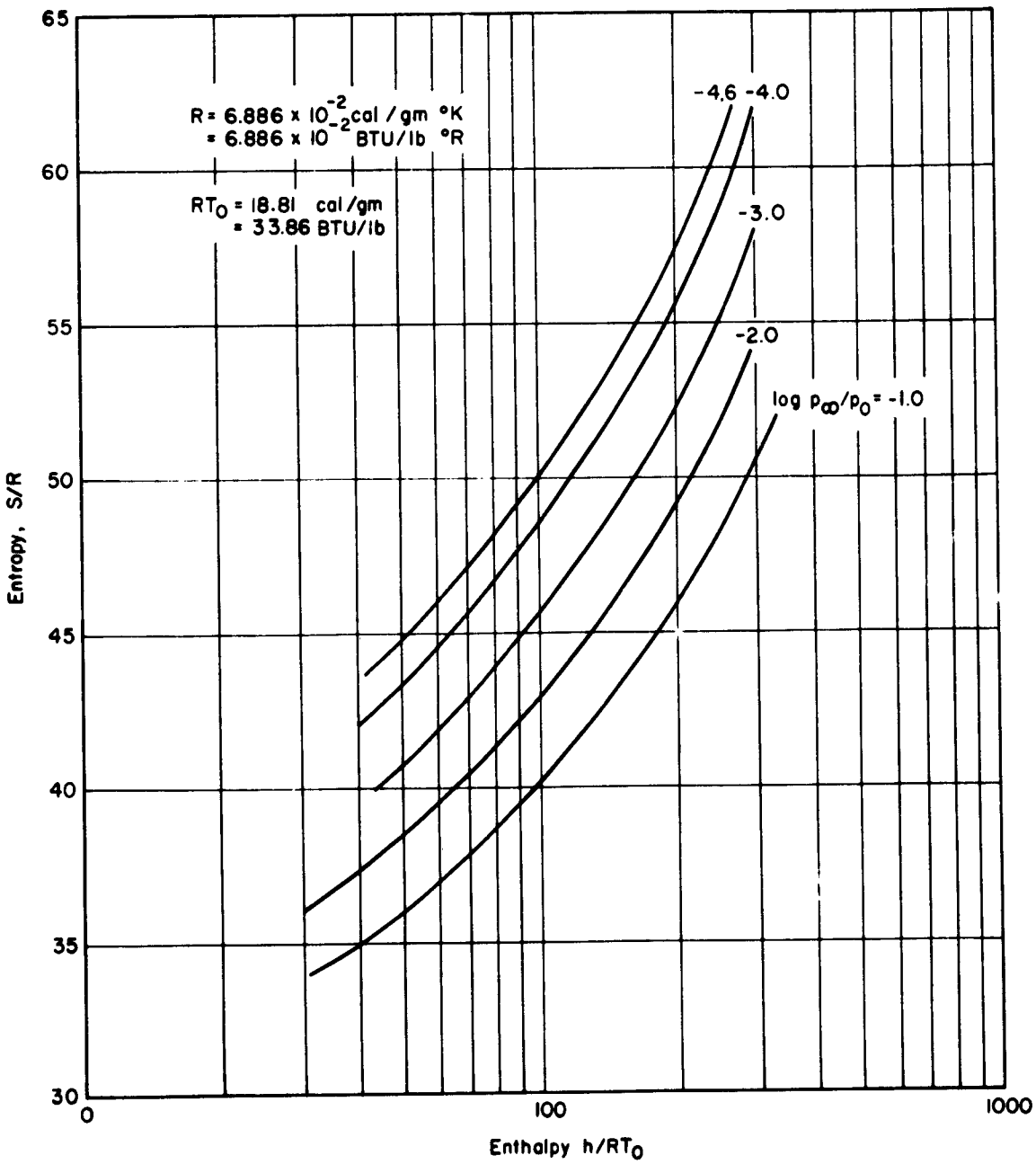

Fig.13 — Entropy

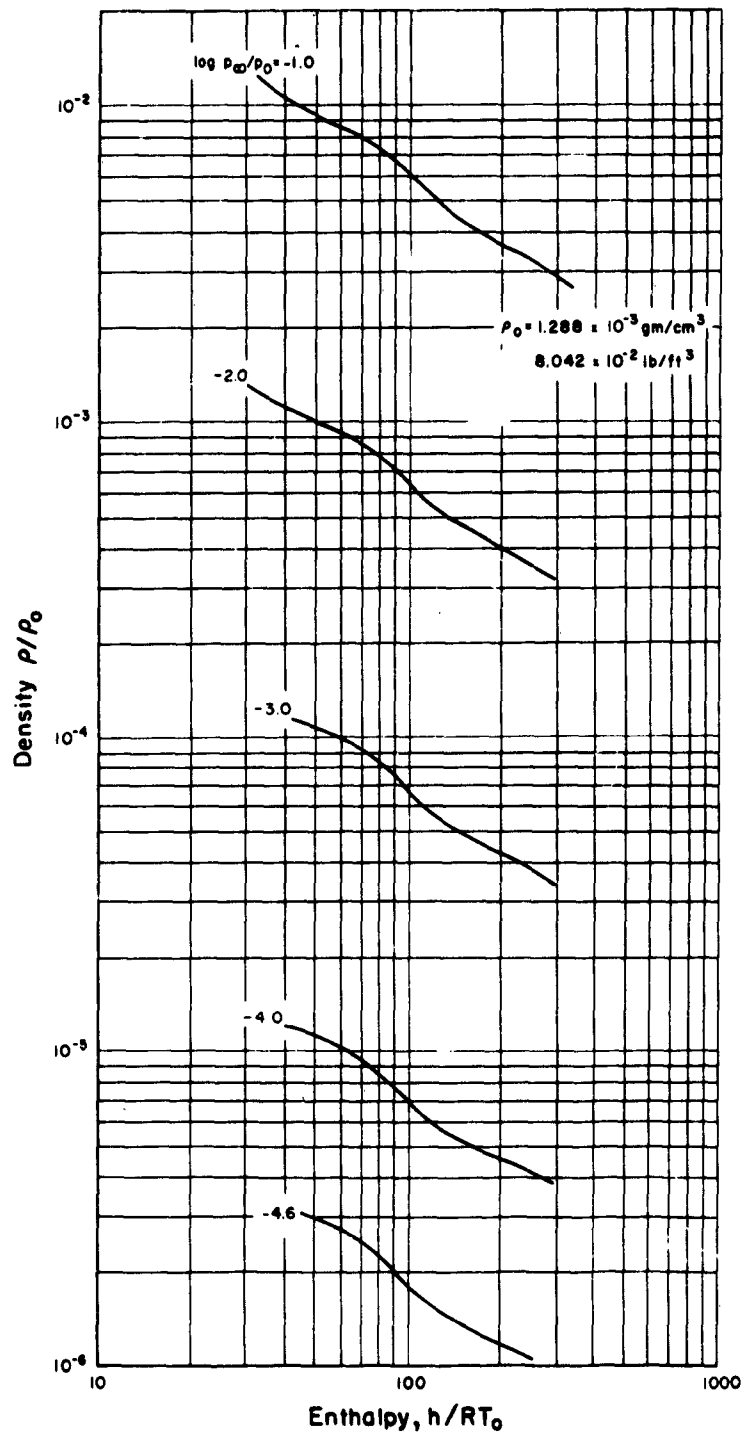

Fig. 14 — Density

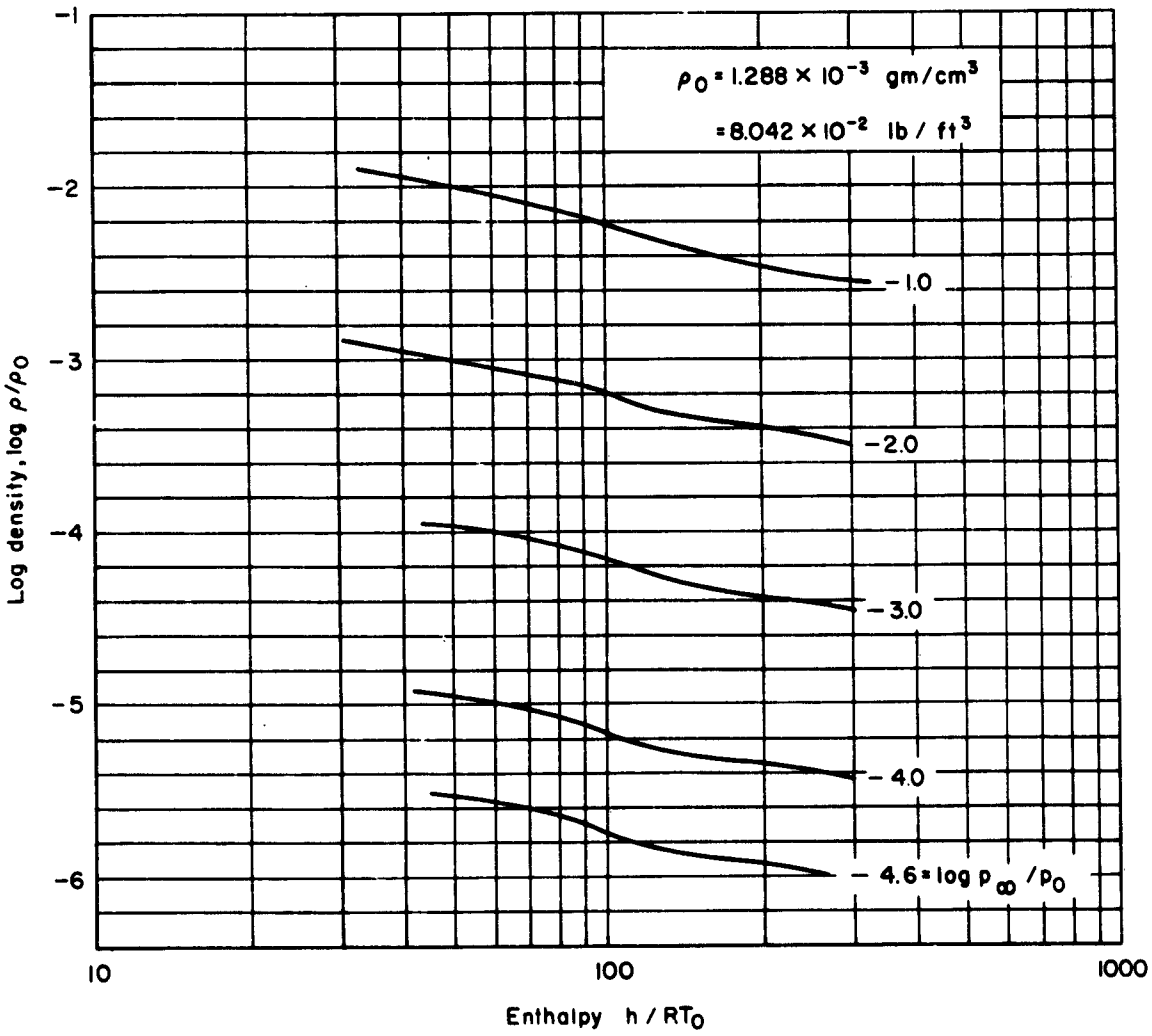

Fig. 15 — Log. density

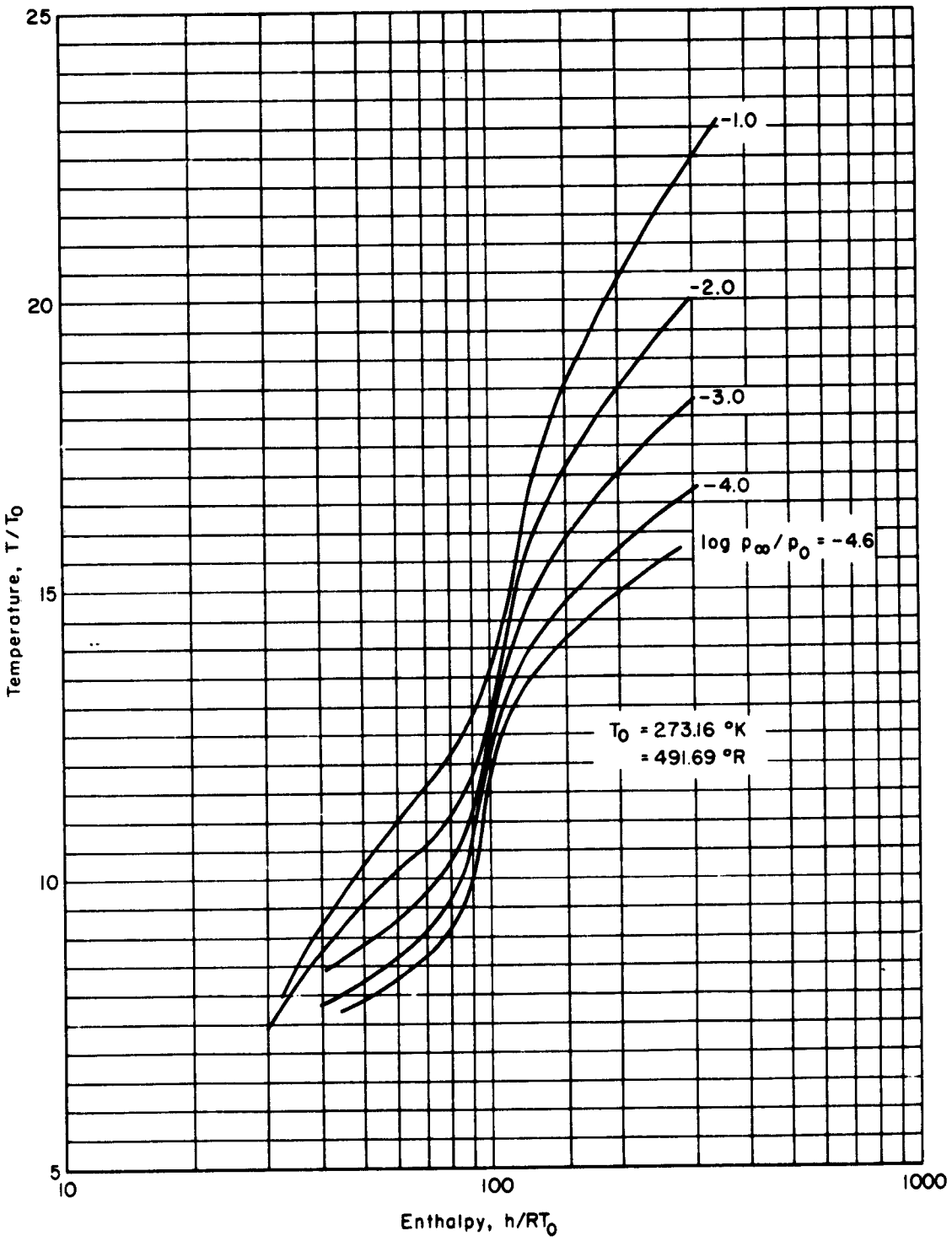

Fig. 16 — Temperature

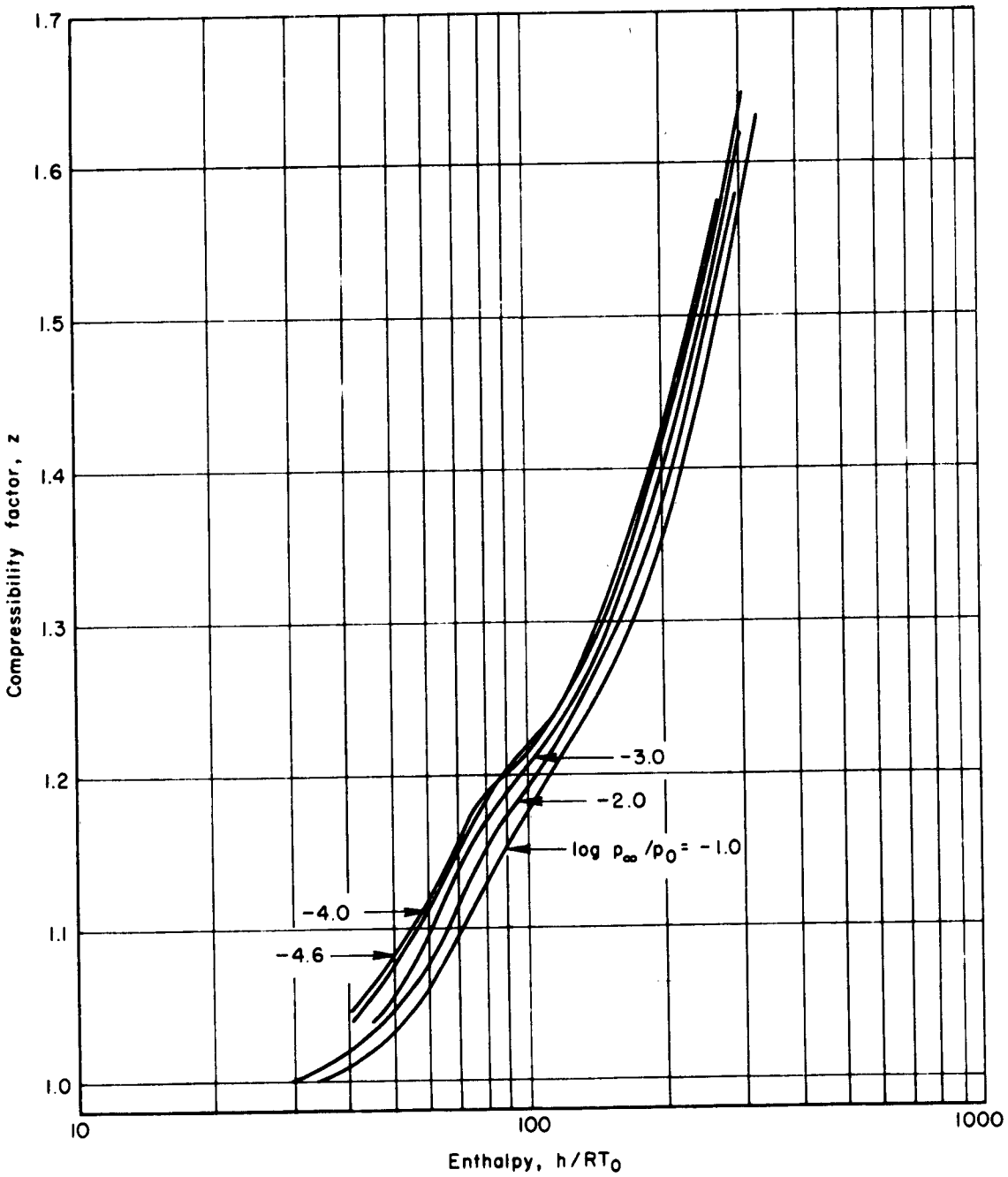

Fig. 17 — Compressibility factor

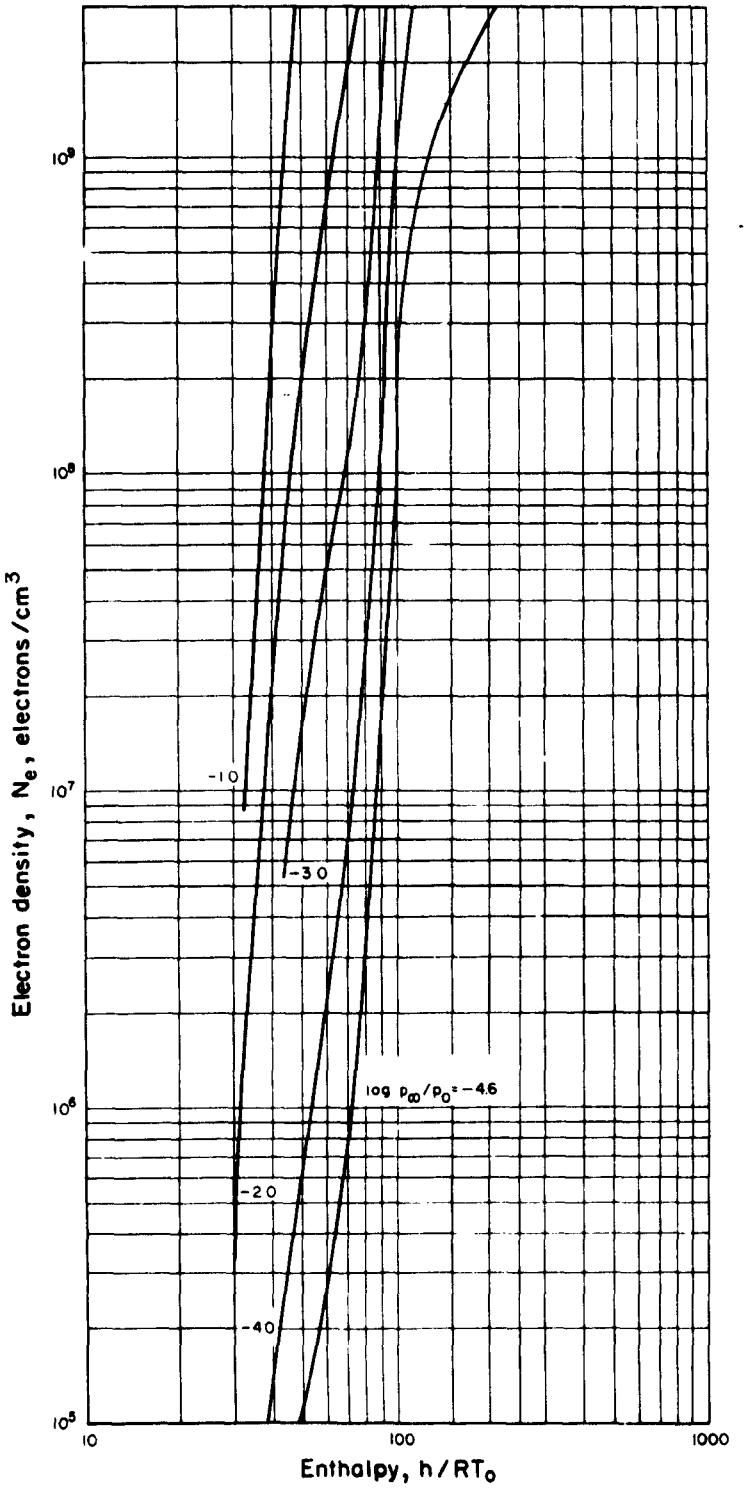

Fig. 18a — Electron density

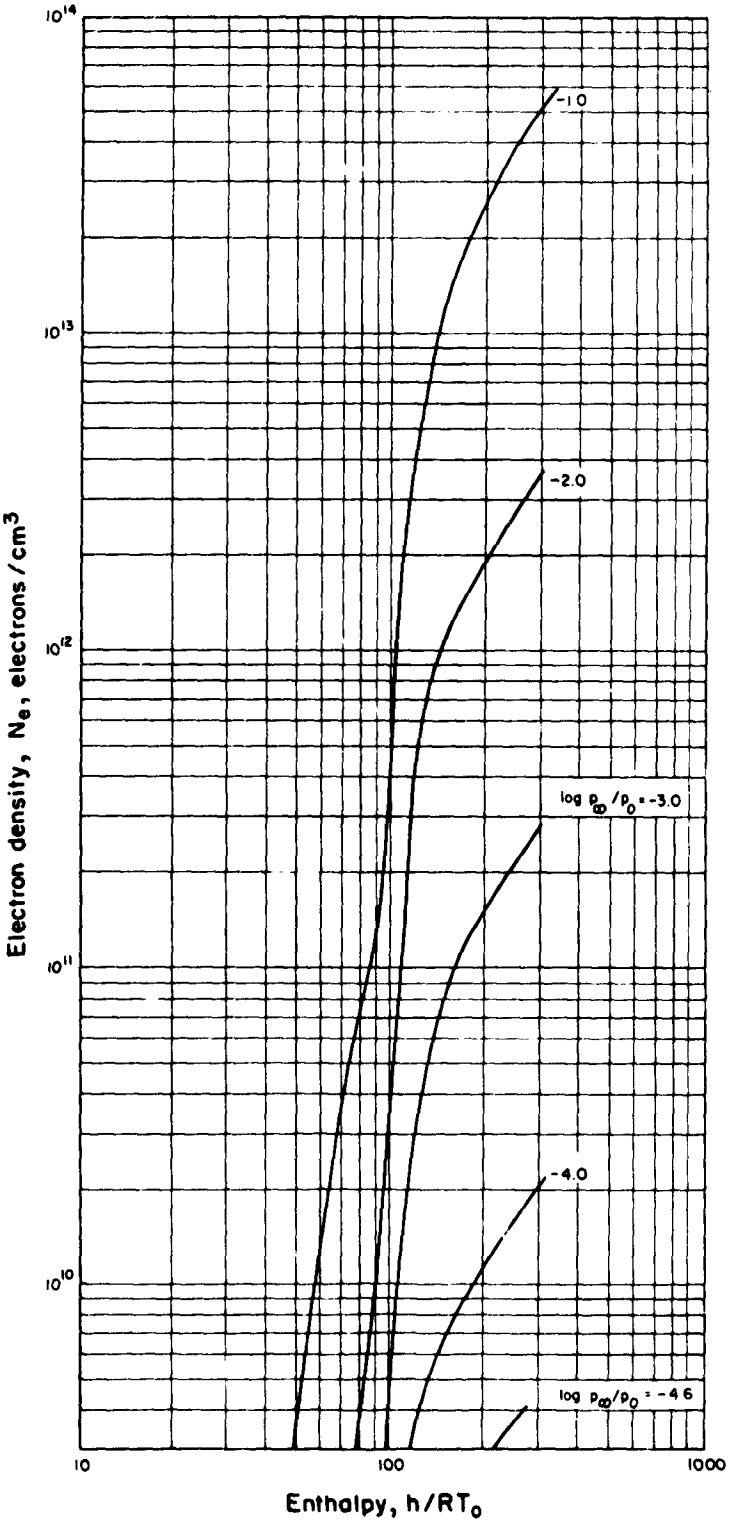

Fig. 18 b — Electron density

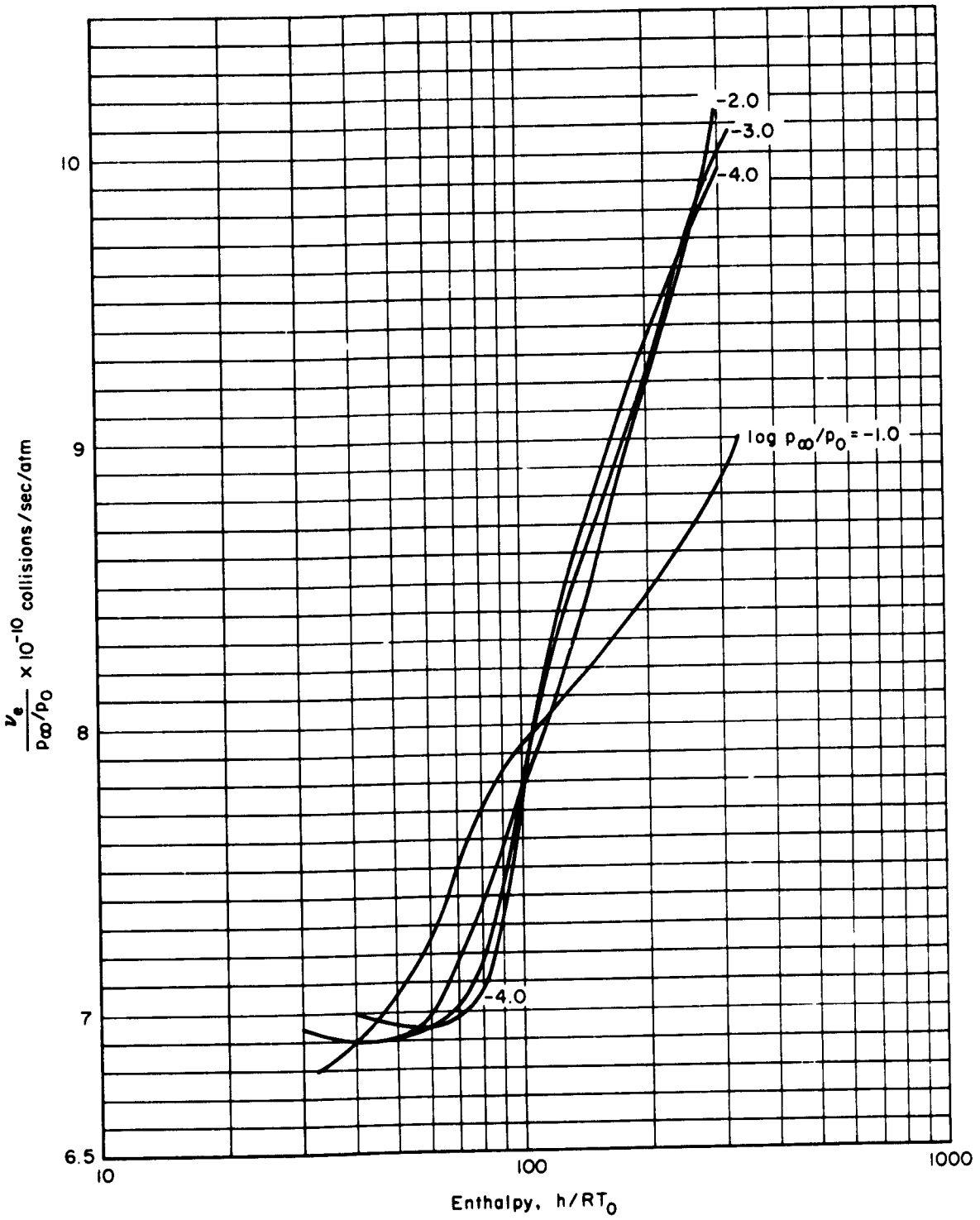

Fig. 19 — Total electron collision frequency (electron-neutral + electron-ion)

REFERENCES

1. Feldman, Saul, "Trails of Axi-Symmetric Hypersonic Blunt Bodies Flying Through the Atmosphere," Journal Aerospace Science, Vol. 28, June 1961, pp. 433-448.

2. Feldman, Saul, Trails of Axi-Symmetric Hypersonic Blunt Bodies Flying Through the Atmosphere, AVCO - Everett Research Laboratory Research Report 82, December 1959.

3. Lykoudis, Paul, Theory of Ionized Trails for Bodies at Hypersonic Speeds, The RAND Corporation, RM-2682-1-PR, October 1961.

4. Lykoudis, Paul, The Growth of the Hypersonic Turbulent Wake Behind Blunt and Slender Bodies, The RAND Corporation, RM-3270-PR, January 1963.

5. Lykoudis, Paul, The Hypersonic Trail in the Expansion-Conduction Region, The RAND Corporation, RM-2818-PR, August 1961.

6. Minzner, R, K. Champion, and H. Pond, "The ARDC Model Atmosphere, 1959," Air Force Surveys in Geophysics, Geophysics Research Directorate, Number 115, August 1959.

7. Feldman, Saul, Hypersonic Gas Dynamic Charts for Equilibrium Air, AVCO - Everett Research Laboratory, Research Report 40, January 1957.

8. Blackwell, F., et al, Properties of Argon-Free Air, Ramo-Wooldridge Corporation, Report GM-TR-76, October 1956.

9. Gilmore, F., Equilibrium Composition and Thermodynamic Properties of Air to 24,000° K, The RAND Corporation, RM-1543, August 1955.